Geology and mineral deposits of the Victorio mining district, Luna County, New Mexico-Preliminary observations

Virginia T. McLemore, Nelia Dunbar, Matt Heizler, and Kelly Donahue
2000, pp. 267-278. https://doi.org/10.56577/FFC-51.267

in:

Southwest Passage: A trip through the Phanerozoic, Lawton, T. F.; McMillan, N. J.; McLemore, V. T.; [eds.], New Mexico Geological Society 51 st Annual Fall Field Conference Guidebook, 282 p. https://doi.org/10.56577/FFC-51

This page is intentionally left blank to maintain order of facing pages.

GEOLOGY AND MINERAL DEPOSITS OF THE VICTORIO MINING DISTRICT, LUNA COUNTY, NEW MEXICO—PRELIMINARY OBSERVATIONS

VIRGINIA T. McLEMORE, NELIA DUNBAR, MATT T. HEIZLER, and KELLY DONAHUE
New Mexico Bureau of Mines and Mineral Resources, New Mexico Institute of Mining and Technology, 801 Leroy Pl., Socorro, NM 87801

Abstract—Three types of mineral deposits (carbonate-hosted Pb-Zn replacement, W-Be-Mo skarn/vein, and porphyry Mo deposits) occur in the Victorio mining district. Some or all of these deposit types may be related to one or more of multiple episodes of igneous activity recognized in the district. Intrusive rocks in the area have been dated using the $^{40}Ar/^{39}Ar$ technique, suggesting a possible intrusion age of around 35 Ma. However, another interpretation of the age data suggests that the intrusive rocks are older than 35 Ma but underwent a reheating event and partial argon loss at around 30–35 Ma. Adularia present in one sample suggests that high-temperature alteration may have taken place at ca. 35 Ma. Within the Victorio district, the carbonate-hosted replacement deposits are epithermal and occur along faults and fractures. Brecciation and dissolution/recrystallization of dolostones are observed associated with the carbonate-hosted replacement deposits. The W-Be-Mo skarn/vein deposits occur within Paleozoic dolostones, limestones, and sandstones. The skarn/vein and porphyry Mo deposits appear to be related to the Victorio granite based on the spatial association and the presence of fluorine-rich phases and Mn-rich garnets in both skarn and granite. Mineralogic and geochemical analysis of the skarns indicate magnesian, rather than calcic, composition. The range of mineral assemblages observed represent both prograde and retrograde phases of skarn formation. The age, genetic relationships, and paragenesis of the carbonate-hosted replacement deposits to the skarn/vein and porphyry Mo deposits are unknown. It is possible that the three types of deposits may be related genetically or that there may have been more than one mineralizing event forming the deposits at different times. A number of questions remain unanswered and will be addressed in future work.

INTRODUCTION

The Victorio (Gage) mining district is located in the southern Victorio Mountains west of Deming in Luna County, New Mexico (Fig. 1) in a stratigraphically and structurally complex area. The area around the Victorio mining district was mapped by Kottlowski (1960, 1963) and Thorman and Drewes (1980). Lone Mountain Mining Co. and Leonard Resources donated subsurface information (Heidrick, 1983), and drill core from the Victorio district to the New Mexico Bureau of Mines and Mineral Resources (NMBMMR). These data and samples improve our understanding of the complex geology of the area, in particular the stratigraphy and structural geology, and insights provided by this new information are presented in this paper.

Lindgren et al. (1910), Holser (1953), Dale and McKinley (1959), Griswold (1961), Griswold et al. (1989), and McLemore et al. (1996) described the Victorio mineral deposits. Three types of mineral deposits occur in the district, including carbonate-hosted Pb-Zn replacement, W-Be-Mo skarn/vein, and porphyry Mo deposits. Although much has been learned about the Victorio district mineralization based on the research listed above, a number of questions remain. These include a rigorous understanding of the mineralogy and geochemistry of the three deposit types, the geochronology of mineral deposits, the presence or absence of genetic relationship between the three types of deposits, and the relationship between mineralization and local igneous rocks. Attempts to answer these questions are addressed in this paper based on new mineralogic, geochemical and geochronological data. Although the data presented here do not answer all of the above questions, they provide some insight into the processes that formed this mineralized area, and provide the foundation on which more detailed studies may be based.

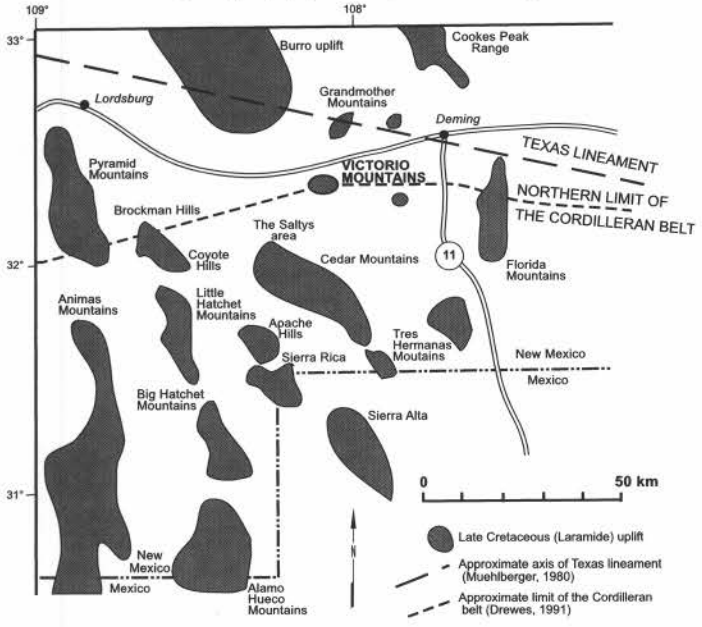

FIGURE 1. Structural features and location of the Victorio Mountains, Luna County, New Mexico.

BACKGROUND

Mining history

The Victorio district was discovered in the late 1800s by three prospectors, William Kent, William Hyters, and J. L. Doughterty and was developed by George Hearst and his partners. George Hearst was father of William Randolph Hearst. The district and surrounding mountains were probably named after Hearst's ranch, Victorio, which may have been named after the Apache war chief. Production of carbonate-hosted Pb-Zn replacement deposits began about 1880, coinciding with the arrival of the Southern Pacific Railroad. Most of the early production (1880–1886) was from the Chance and Jessie mines where $800,000–$1,600,000 worth of lead, zinc, and silver were produced by Hearst (Fig. 2; Jones, 1904; Lindgren et al., 1910). The Gage Mining Co. controlled most of the mines on Mine Hill in 1914. The Victorio Mining Co. operated the Jessie and Chance mines in 1936–1940.

Beryllium and tungsten vein and skarn deposits were discovered in the Victorio Mountains in the early 1900s (Griswold, 1961; Holser, 1953; Dale and McKinney, 1959). Tungsten was produced from 1942 to 1944 from the mines at Tungsten Hill (Fig. 2). In 1942, approximately 20,000 short tons (st) of ore containing an average of 1% WO_3 and worth nearly $70,000 were produced from the Irish Rose claim (Dale and McKinney, 1959). The ore contained mostly scheelite with some galena, smithsonite, and helvite. In addition, 19.6 st of 60% WO_3 were produced from the mine in later years.

Mining continued in the district sporadically until 1957, mostly from the carbonate-hosted Pb-Zn replacement deposits (Table 1). Total production is estimated as 70,000–130,000 st of ore mined between 1880 and 1957, which yielded approximately $2.3 million worth of lead, zinc, silver, gold, and copper, including 17.5 million lbs Pb and >60,000 lbs Zn (Table 1; McLemore and Lueth, 1995, 1996; McLemore et al., 1996). Limestone was also quarried for aggregate for highway con-

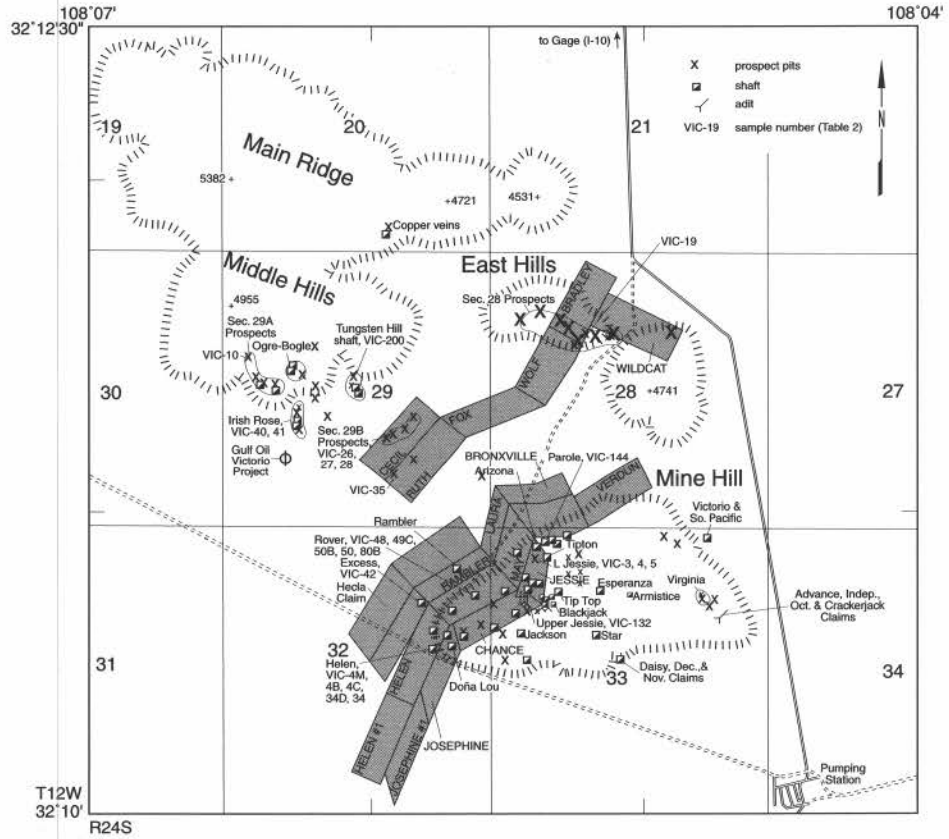

FIGURE 2. Mines, prospects, and sample locations in the Victorio district.

struction.

Most of the workings are on Mine Hill in the southern part of the Victorio Mountains (Fig. 2), coinciding with the area of significant production from carbonate-hosted Pb-Zn replacement deposits (Griswold, 1961). Several shafts are 84 m deep and underground workings are extensive (Griswold, 1961; V. T. McLemore, unpublished field notes, December 1993). Most of these workings were closed by the New Mexico Abandoned Mine Lands Bureau in 1994. The W-Be-Mo skarn/vein deposits are found in the Middle Hills north of Mine Hill.

Exploration since the 1950s has been modest; most companies were exploring for porphyry copper deposits. In 1969–1970, Humble Oil Co. drilled four holes and encountered skarns, but they did not find any significant porphyry copper deposits. Keradamex drilled two holes in 1971 without encountering any significant mineralized zones. Asarco, Rosario Exploration, Southern Union Co., Newmont, Donegan and Donegan, Leonard Resources, and Bethlehem Copper Corp. also examined the area. Gulf Minerals Resources, Inc. drilled 71 holes in 1977–1983 and delineated a porphyry Mo and Mo-Be-W skarn deposit northwest of Mine Hill and south of Middle Hills (Fig. 2). At a cut-off grade of 0.02% WO_3, resources were estimated as 57,703,000 st of 0.129% Mo and 0.142% WO_3. Open pit resources were estimated as 11,900,000 st of 0.076% WO_3 and 0.023% Be (Bell, 1983). In 1987–1988, Cominco American Resources examined the district for gold potential and drilled 15 holes on and around Mine Hill, and found minor intercepts of mineralized zones. Santa Fe Pacific Mining, Inc., drilled 18 holes in 1990–1991 and Echo Bay Exploration, Inc., drilled 8 holes in 1993. Gage Mining Co. owns most of the patented claims on Mine Hill and the Middle Hills is mostly federal land.

Regional geology

Lower Cretaceous sedimentary rocks in southwestern New Mexico, including those in the Victorio Mountains, were deposited in an extension of the Chihuahua basin (Mack et al., 1986). The Victorio Mountains are on the southwestern edge of the Laramide Burro-Florida uplift (Elston, 1958; Turner, 1962; Mack and Clemons, 1988). During the Laramide (Late Cretaceous–Eocene), this area underwent compressional deformation as a result of the collision of the North American and Farallon plates (Drewes, 1991). This belt of compressional deformation extended from El Paso, Texas westward to Las Vegas, Nevada and is called the Cordilleran orogenic belt. The Victorio Mountains form the northern edge of this Laramide belt as defined by Drewes (1991). This deformation belt (eastern intermediate zone of Drewes, 1991) in southwestern New Mexico is characterized by folding and thrusting of older rocks and local detachment along the crystalline basement.

The Victorio Mountains also lie near the Texas lineament (Fig. 1) which extends from Trans-Pecos Texas west-northwestward into southeastern Arizona where it probably joins the Arizona transitional zone (Muehlberger, 1980; Wertz, 1970a, b). It is a prominent 80–150 km wide zone that is defined by basins, ranges, and structural features (Lowell, 1974; Wertz, 1970a, b; Turner, 1962; Schmitt, 1966; Drewes, 1991). Dip-slip (normal, steep reverse or thrust) movements are common throughout this zone and locally strike-slip movement has been documented (Turner, 1962; Wertz, 1970a, b; Muehlberger, 1980; McLemore, 1993).

METHODOLOGY

This study incorporates new mineralogic, geochemical, and geochronological data with published and unpublished studies of the geology and mineral deposits of the Victorio Mountains. Current studies by the authors include detailed remapping and sampling of the rocks. Approximately 6 km^2 are being mapped in detail at a scale of 1:12,000 using standard U.S. Geological Survey (USGS) 7½-minute topographic quadrangle maps (Gage and Gage NW; Fig. 3). Cross-sections were compiled using company drill data and surface mapping (Fig. 4). Mineralized samples were collected and analyzed. Some samples were analyzed at the USGS by inductively coupled plasma-atomic emission spectrometry (ICP-AES). Other samples were analyzed by flame atomic-absorption spectrophotometry (FAAS) at the NMBMMR using four-acid digestion and Au and Ag was by fire assay.

Samples collected from drill cores were examined using a Cameca SX-100 electron microprobe at NMIMT. Three types of analyses were performed, including (1) imaging of sample textures and textural rela-

TABLE 1—Reported metal production from the Victorio district, Luna County (from U.S. Geological Survey, 1902–1927; U.S. Bureau of Mines, 1927–1990; Griswold, 1961). — none reported.

YEAR	ORE (ST)	COPPER (LBS)	GOLD (OZ)	SILVER (OZ)	LEAD (LBS)	ZINC (LBS)	TOTAL VALUE ($)
1880–1903	—	—	—	—	—	—	1,150,000
1904	274	—	—	2047	76,465	—	6170
1905	—	—	—	—	—	—	—
1906	620	—	19.98	2876	186,000	—	12,971
1907	1200	—	—	3600	408,000	—	24,992
1908	—	—	—	—	—	—	—
1909	183	1069	—	2460	85,418	—	5381
1910	22	—	—	267	21,318	—	1085
1911	180	1598	5.03	883	66,250	—	3753
1912	2123	—	275.11	23,305	684,867	7865	51,382
1913	3895	58	536.24	40,416	902,781	—	75,227
1914	132	—	—	552	35,599	—	1851
1915	216	2320	—	1476	53,958	—	4147
1916	1804	—	171.01	8436	381,000	—	35,375
1917	1505	270	—	11,301	428,907	—	51,449
1918	1631	—	—	14,358	323,493	—	45,497
1919	1728	538	238.30	10,438	356,775	—	35,626
1920	1331	1641	—	10,167	298,113	—	41,894
1921	676	—	71.98	4709	144,467	—	12,698
1922	158	—	—	583	28,622	—	2529
1923	468	1028	62.89	2195	64,930	—	7796
1924	285	—	—	485	47,975	—	4295
1925	609	1000	—	2833	116,600	—	13,075
1926	129	—	7.20	633	22,500	—	2344
1927	28	—	—	224	7398	—	638
1928	40	—	—	188	9000	—	717
1929	278	284	—	1004	27,000	—	2516
1930–1934	—	—	—	—	—	—	—
1935	40	—	5.60	259	4900	—	578
1936	<1	—	—	11	100	—	14
1937	1009	2815	93.40	3589	67,000	—	10,339
1938	3595	6000	397.4	13,283	210,000	—	32,744
1939	3493	8700	453	16,802	278,800	—	41,269
1940	903	2600	113	3981	78,700	—	11,015
1941–1946	—	—	—	—	—	—	—
1947	1509	2400	24	2535	107,800	42,600	24,316
1948	119	—	1.0	347	18,000	—	3571
1949	—	—	—	—	—	—	—
1950	73	—	1.0	275	6000	—	1094
1951–1954	—	—	—	—	—	—	—
1955	57	—	1	175	2000	—	491
1956	—	—	—	—	—	—	—
1957	53	—	—	239	4809	2000	1134
TOTAL 1904–1957	30,367	32,271	2477.14	186,882	6,233,492	52,465	569,973
ESTIMATED TOTAL 1880–1959	70,000–130,000	41,000	12,200	581,500	17,500,000	>60,000	2,330,700

tionships, (2) qualitative and (3) quantitative analysis of mineral phases. In this report, the imaging and qualitative analyses will be discussed, whereas quantitative results will be discussed elsewhere. Instrumental conditions of 15 kV accelerating voltage, 20 nA beam current, and a 1-μ-beam size were used.

Ages of four samples were determined using the $^{40}Ar/^{39}Ar$ method at the New Mexico Geochronological Research Laboratory at NMBMMR. Biotite and K-feldspar pairs from two Victorio granite samples and groundmass concentrates from a mafic sill and dacite flow were analyzed by the furnace incremental-heating age-spectrum method. Laboratory procedures are briefly described by McLemore et al. (1999) or can be obtained from the senior author.

LOCAL GEOLOGY

Stratigraphy

Kottlowski (1960, 1963) mapped the geology of the Victorio Mountains (Figs. 3, 4) and established the stratigraphy of the Paleozoic

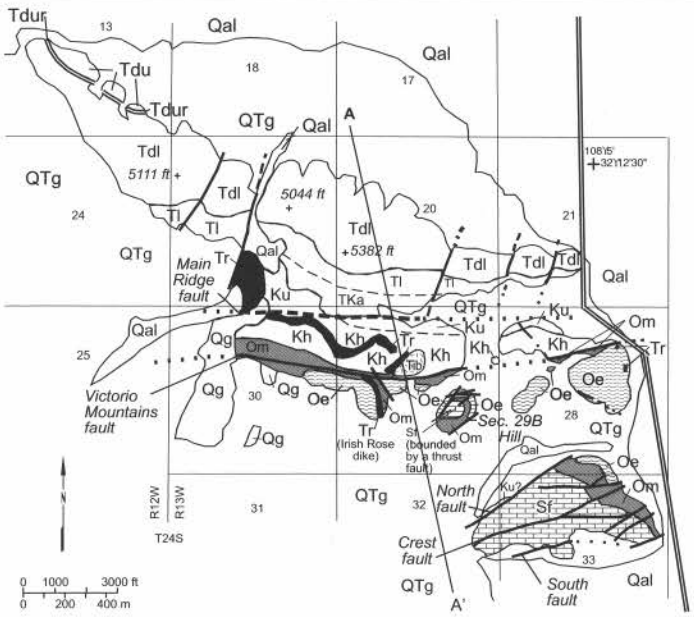

FIGURE 3. Simplified geologic map of the Victorio Mountains (modified from Kottlowski, 1960, 1963; Thorman and Drewes, 1980; unpublished mapping by Gulf Resources, Inc.; unpublished mapping by V. T. McLemore). Line A–A' is shown in Figure 4. Symbols explained in Figure 5.

section (Fig. 5). Thorman and Drewes (1980) remapped the geology and established tentative correlation between the Cretaceous sedimentary rocks of Kottlowski (1960) with the Bisbee Formation (sic) (Fig. 5). Lucas et al. (2000) correlated the Cretaceous sedimentary rocks to the U-Bar and Hell-to-Finish formations. Lawton and Clemons (1992) correlated the sedimentary rocks overlying the U-Bar and Hell-to-Finish formations to the Lobo Formation. This report, using subsurface data not available to the previous workers (presented in Heidrick, 1983), recognized additional Cretaceous–Tertiary intrusive rocks and described the subsurface Proterozoic lithologies and Bliss Formation. A summary of the stratigraphic relationships is in Table 2.

Proterozoic rocks and the Cambro-Ordovician Bliss Formation were encountered in drill cores from the Victorio district despite not being exposed at the surface (Fig. 4). Proterozoic rocks consist of quartzo-feldspathic gneiss and amphibolite. The quartzo-feldspathic gneiss consists of alternating metamorphosed siltstone, sandstone, and arkose layers. The amphibolite is composed of calcic plagioclase, hornblende, and biotite and shows weak to moderate contorted foliation. The texture of the amphibolite ranges from fine-grained foliated biotite schist to coarse-grained diabase (Heidrick, 1983). In the subsurface, the Bliss Formation is variable in thickness, ranging from 32 to 42 m (Fig. 4; Heidrick, 1983). The Bliss Formation lies unconformably on Proterozoic basement with a 1-m thick basal conglomerate consisting of subangular–subrounded Proterozoic metamorphic rocks and quartz pebbles in a fine sand matrix. The next 4–7 m is typically a clean orthoquartzite. The upper 26 m of the Bliss Formation has two distinct lithologies, a silty quartzite unit and a limy to dolomitic siltstone. In drill core, both of these lithologies host significant W-Be-Mo skarn/vein deposits.

The oldest rocks exposed at the surface in the area are Ordovician thin- to medium-bedded limestones, dolostones, and calcarenites with chert interbeds of the El Paso Group, which is 152–165 m thick at the surface and may exceed a thickness of 300 m in the subsurface (Figs. 3, 4; Kottlowski, 1960, 1963; Thorman and Drewes, 1980). In the drill core, the total thickness is difficult to determine because of alteration, disruption by igneous intrusions, and faulting (Fig. 4). The El Paso Group consists of three formations; Hitt Canyon, McKelligan, and Padre formations. Locally in the drill core, these different formations are distinquishable, but in most drill holes the alteration is too intense to define adequately the contacts between them. In the Victorio Mountains, the El Paso Group contains local gastropods, cephalopods, and algal masses. Although in many areas, the contact between the El Paso Group and the Bliss is arbitrary, and the Ordovian Montoya Group lies slightly unconformably on the El Paso Group. Locally, the El Paso Group unconformably overlies the Bliss Formation in the subsurface and is conformably overlain by the Montoya Group.

TABLE 2. Stratigraphic relationships in the Victorio Mountains.

Tertiary–Late Cretaceous?
- Basalt to andesite dikes and sills (alteration age of 35 Ma, $^{40}Ar/^{39}Ar$)
- Tungsten Hill intrusive breccia pipe
- Rhyolite and dacite porphyry dikes, including the Irish Rose rhyolite porphyry (24.8 Ma, fission track)
- *Victorio granite (either 70 or 35 Ma, $^{40}Ar/^{39}Ar$)
- Quartz latite/rhyolite porphyry dikes
- Porphyritic andesite-basalt dikes
- Victorio Peak dacite (41.7 Ma, fission track)
- Lobo Formation (210–275 m)
- Dacite flows and flow breccias (Hidalgo Formation?) (0–30 m)

Cretaceous
- Bisbee Group (121–213 m)
  - U-Bar Formation (119 m)
  - Hell-to-Finish Formation (73 m)

Silurian
- Fusselman Dolomite (152–274 m)

Ordovocian
- Montoya Group (91 m)
  - Cutter Dolomite (15–61 m)
  - Aleman Formation (45.7 m)
  - Upman Dolomite (21.3 m)
    - *Cable Canyon Sandstone (1.5–6.1 m)
- El Paso Group (365 m)
  - *Padre Formation
  - *McKelligan Formation
  - *Hitt Canyon Formation

Ordovician–Cambrian
- *Bliss Formation (29–38 m)

Proterozoic
- *Amphibolite (metadiabase)
- *Quartzo-feldspathic gneiss (granite)

* found only in drill core

In the Victorio Mountains, the Montoya Group is 90–113 m thick and consists of fine- to medium-grained crinoidal limestones and dolostones (Kottlowski, 1960) in four formations (from oldest to youngest): Cable Canyon Sandstone, Upham Dolomite, Aleman Formation, and Cutter Dolomite (Kottlowski, 1960; Thorman and Drewes, 1980). The Cable Canyon Sandstone is difficult to recognize at the surface in the Victorio Mountains and may be a sandy limestone that is indistinguishable from the overlying basal Upham Dolomite. In drill core, the Cable Canyon Sandstone is a fine-grained quartz sandstone to sandy limestone. The Upham Dolomite consists of dark gray, medium-bedded dolostone and is characterized by crinoids. The Aleman Formation consists of dark gray, medium-bedded dolostone with chert interbeds. The Cutter Dolomite consists of gray, thinly-bedded dolostone to dolomitic lime-

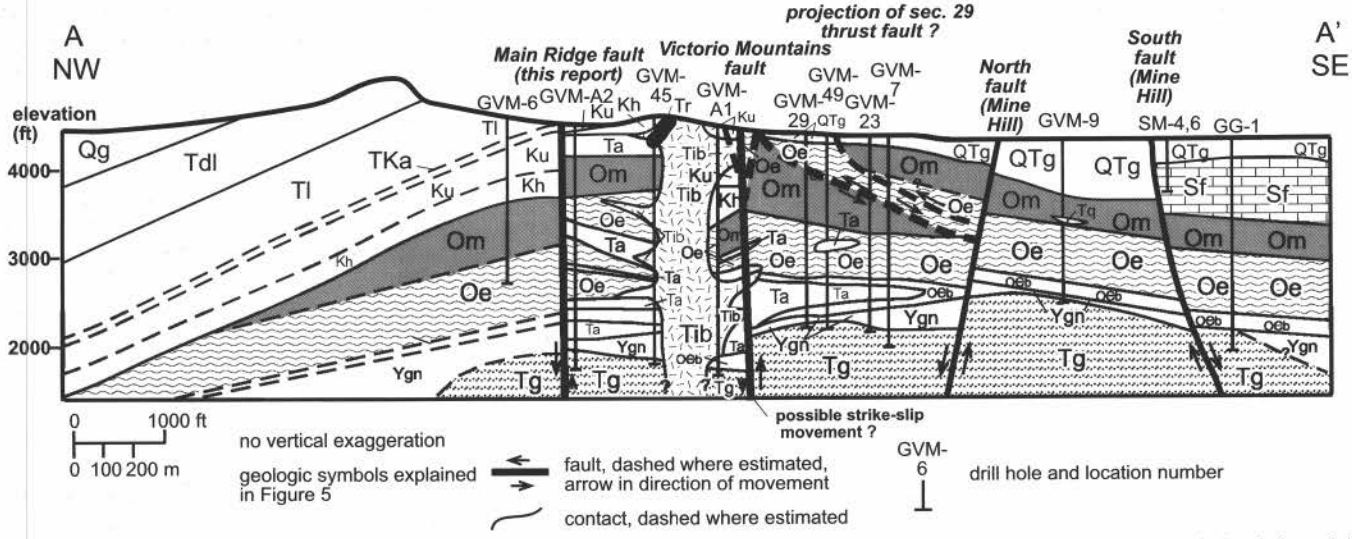

FIGURE 4. Simplified cross section of the Victorio Mountains (modified from company drill data and unpublished mapping by V. T. McLemore). Symbols explained in Figure 5. Some of the drill holes are projected onto the cross-section.

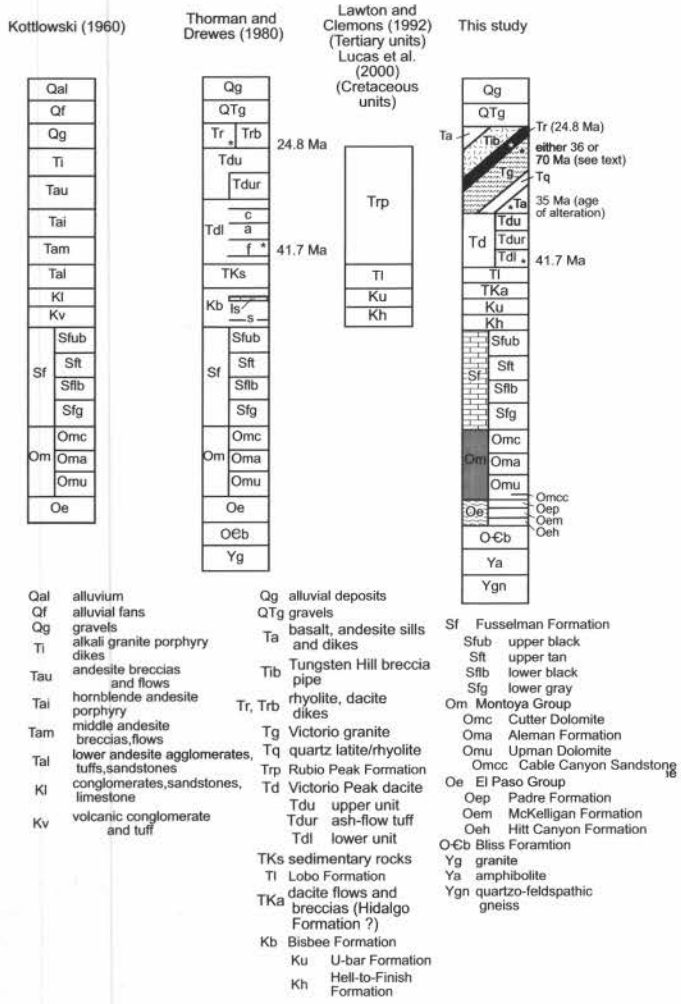

FIGURE 5. Revisions of the stratigraphic relationships in the Victorio Mountains (from Kottlowski, 1960, 1963; Thorman and Drewes, 1980; Lawton and Clemons, 1992; Lucas et al., 2000; unpublished mapping by V. T. McLemore).

stone with shale interbeds.

The Silurian Fusselman Dolomite lies conformably on the Montoya Group and consists of 10–300 m of fine- to coarse-grained dolostone, which is commonly divided into four informal units (from oldest to youngest): gray, lower black, tan, and upper black members (Kottlowski, 1960). The lower gray unit is a gray, sandy dolostone. The lower black unit consists of dark gray to black, dolostone containing abundant corals and minor chert. The tan and lower black members are massive dolostones. The top half of the Fusselman Dolomite is abundant in chert beds. Brachiopods are locally abundant. The Victorio Mountains contain one of the western-most outcrops of the Fusselman Dolomite (Thorman and Drewes, 1980). The Fusselman Dolomite is thickest at Mine Hill and thins to the north. Thorman and Drewes (1980) map Fusselman outcrops north of the Victorio Mountain fault; however, these outcrops are interpreted to belong to the Hell-to-Finish Formation (V. T. McLemore, unpublished mapping). A major angular unconformity separates the marine Paleozoic rocks from the subaerial Lower Cretaceous rocks (i.e., Bisbee Group).

Lucas et al. (2000) correlated the Lower Cretaceous Bisbee Group sediments to the Hell-to-Finish and U-Bar formations on the basis of rare fossils, lithologies, and stratigraphic sections. The oldest unit is the Hell-to-Finish Formation that consists of a maximum of 73 m of interbedded conglomerate, conglomeratic sandstone, calcarenite, and mudstone. The conglomerates contain either (1) limestone and chert clasts or (2) quartzite clasts. The overlying U-Bar Formation, with a maximum of 119 m, consists of a lower oyster-bearing limestone, middle sandstone and quartz-pebble conglomerate, and an upper calcarenite and grainstone. Lucas et al. (2000) divided the U-Bar Formation in the Victorio Mountains into three members: Carbonate Hill (oldest), Victorio Mountains, and Still Ridge members (youngest).

A sequence of conglomerate, sandstone, siltstone, and volcanic flows and breccias 240–305 m thick conformably overlies the U-Bar Formation. Purple to maroon to gray dacite flows and flow breccias occur at the base that may correlate with the Hidalgo Formation (~71 Ma) exposed in the Little Hatchet Mountains (Lawton et al., 1993; Young et al., this volume). The dacite flows and flow breccias (~30 m thick) are overlain by clastic sedimentary rocks that Lawton and Clemons (1992) correlated to the Eocene Lobo Formation (210–275 m thick). The conglomerate is more prevalent in the upper part of the sequence and consists of angular to rounded granite, dacite, andesite, marble, limestone, and quartz clasts, as much as 10 cm long.

The Main Ridge of the Victorio Mountains is made up of Tertiary volcanic and volcaniclastic rocks, called the Victorio Peak dacite, which unconformably overlies the Lobo Formation. The Victorio Peak dacite consists of approximately 300–500 m of agglomerates, flow breccias, tuffs, and dacite lavas, including a 41.7 ± 2-Ma dacite breccia (zircon, fission track; Thorman and Drewes, 1980). A 1–2-m thick, white–light gray, rhyolitic ash-flow tuff crops out in the upper part of the Victorio Peak dacite, north of the microwave towers. Ash-flow tuffs also make up South Hills, south of the mapped area shown in Figure 3. If the fission track age is correct, then the Victorio Peak dacite is correlative with the Rubio Peak Formation.

The Victorio granite is believed to be Late Cretaceous or Tertiary, as discussed below. It is found only in the subsurface. Based on petrographic observation, it is medium–coarse grained and consists of K-feldspar, plagioclase, quartz, biotite, muscovite, with trace pyrite, scheelite, apatite, garnet, fluorite, and zircon. The southern portion of the granite is a two-mica (muscovite and biotite) granite, whereas the northern portion is a biotite granite. The Victorio granite mostly intrudes Proterozoic rocks, but also cuts the Bliss Formation in two drill holes (Fig. 4). Furthermore, there are several rhyolite dikes that branch upward from the main granitic body. The Victorio granite is mostly unaltered with only small amounts of weak argillic to weak phyllic alteration. One sample of granite from the Victorio Mountains area was examined using the electron microprobe, and, as observed petrographically, contains an assemblage of quartz, K-feldspar, biotite, plagioclase, and magnetite. However, in addition to these phases, the granite contains abundant, pinkish, Mn-rich garnets that include an abundance of heavy-mineral inclusions as well as fluorite (Fig. 6). These inclusions include Hf-rich zircon, and Th-, U- and Y-rich allanite. These heavy-mineral inclusion phases appear to have crystallized from the granitic magma, as does the fluorite. The abundance of these phases, as well as the presence of primary fluorite included in garnet, suggests that the Victorio granite is anomalously enriched in heavy elements, as well as fluorine. Molybdenite and scheelite also have been found in the Victorio granite.

Sills and steeply dipping dikes of basalt, andesite, dacite, and rhyolite porphyry intruded the Paleozoic and Cretaceous sedimentary rocks, especially in the Middle Hills area (Fig. 4). The altered Irish Rose rhyolite porphyry dike at the Irish Rose mine in the Middle Hills is nearly flat lying, but cuts bedding in the limestone and dolostone. An altered rhyolite dike intruded a fault at the Rambler-Excess mines at Mine Hill (Griswold, 1961). Altered andesite and rhyolite dikes also intruded the limestones and dolostones on East Hills. Numerous basalt, andesite, dacite, and rhyolite dikes and sills intruded the Paleozoic limestones and dolostones in nearly all of the drill holes in the Victorio district; most are altered. The age relationships between the igneous intrusions are uncertain (Fig. 5) and will be addressed in future work.

A breccia pipe crosscuts the limestone in the Middle Hills (Figs. 3, 4). It consists of angular and brecciated fragments of quartz, quartz sandstone, conglomerate, limestone, granite, marble, andesite, rhyolite, and quartzo-feldspathic gneiss, and is cemented mostly by quartz, rock flour, and hematite. Based on the presence of what are interpreted to be granite fragments in the breccia pipe, the breccia pipe is thought to be

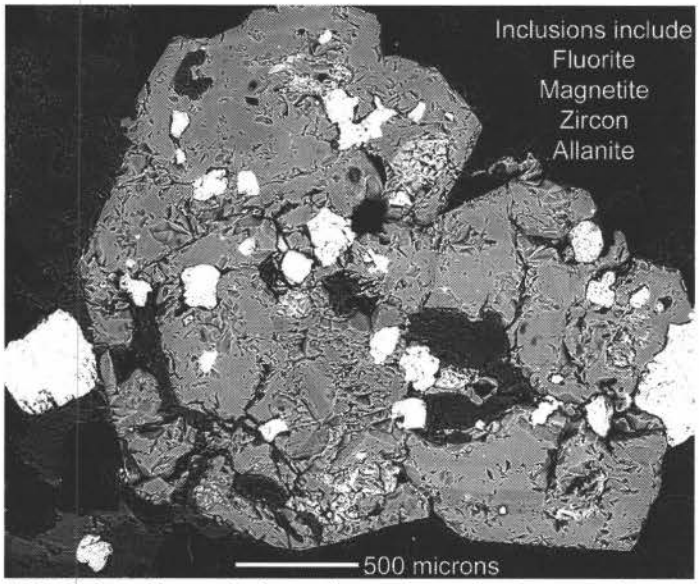

FIGURE 6. Backscattered electron image of a Mn-bearing garnet from the Victorio granite with inclusions of fluorite, magnetite, zircon and allanite. The garnet is the medium-gray phase that fills the field of view. The dark-gray inclusions in the garnet are fluorite, and the brighter inclusions are the magnetite, zircon and allanite.

related to a late stage of Victorio granite crystallization. Quartz veins, some of which contain trace amounts of pyrite and possibly molybdenite, locally cut the breccia pipe. A rhyolite dike intruded the breccia pipe and was dated as 24.8 Ma (fission track, zircon, Thorman and Drewes, 1980). These field relationships indicate that rhyolite intrusion occurred before and after formation of the breccia pipe and that the breccia pipe is younger than the marble formation.

Structural geology

Rocks in the Victorio Mountains dip gently to moderately to the north or south and are offset by faults (Fig. 4). Folded sedimentary rocks are present locally. The type and extent of faulting in the Victorio Mountains remains poorly constrained and will be addressed in more detail in future work.

An east–west fault separates the Middle Hills from the Main Ridge and is called the Main Ridge fault in this report (Fig. 3). This fault is not well exposed and forms drainages north of the Middle and East Hills. The fault separates shallow-dipping (<15°) U-Bar and Hell-to-Finish sedimentary rocks from more steeply dipping (20–30°) dacite flows and flow breccias (Hidalgo Formation?) and sedimentary rocks of the Lobo Formation (Fig. 4). In the saddle between the Middle Hills and Main Ridge, the fault is characterized by near vertical fractures.

The steeply dipping Victorio Mountains fault is exposed in both the East and Middle Hills and juxtaposed northeast-dipping sedimentary rocks of the U-Bar and Hell-to-Finish formations against south- or west-dipping Ordovician limestones (Fig. 3). The fault is locally sinuous and consists of numerous splays that are also steeply dipping. The Victorio Mountains fault has been interpreted as a strike-slip or polyphase normal fault (Thorman and Drewes, 1980), as a reverse fault (Kottlowski, 1960; Griswold, 1961), and as a thrust fault (Corbett and Woodward, 1970). Possible strike-slip movement along the fault is evidenced by the abrupt thinning of the Fusselman Dolomite between Mine Hill and the Central Hills, and then the lack of any Fusselman north of the fault. Alternatively, this pattern may be caused by post-Silurian erosion on the south edge of the Burro uplift. The Middle Hills along and south of the east–west-trending Victorio Mountains fault is complexly faulted (Figs. 3, 4). Numerous northeast-trending, high-angle normal faults cut the hills; many are splays of the Victorio Mountains fault. Numerous shafts and prospect pits expose the faults, which vary from narrow fracture zones to diffuse brecciated zones that are typically <1 m wide. A breccia pipe intruded along a splay of the Victorio Mountains fault, suggesting that the fault is older than the intrusive activity. All of the known mineralizied zones occur at or south of the fault; only minor copper veins are found north of the Victorio Mountains fault.

The Upham Dolomite unconformably overlies the El Paso Group on Section 29B Hill (Fig. 3). The contact is not well exposed and is mapped at the first dark-gray dolostone. A low-angle thrust fault separates the Fusselman Dolomite, which caps the top of the Section 29B Hill from the underlying Upham Dolomite. The Fusselman Dolomite is approximately 33 m thick, whereas the Upham Dolomite is approximately 27 m thick. Several northeast-trending normal faults cut the thrust fault and the limestones. These relationships indicate that thrust faulting occurred prior to normal faulting.

Mine Hill is also extensively faulted. The North fault (Mine Hill Windmill fault of Thorman and Drewes, 1980) strikes N50–70°E and forms the northern boundary of Mine Hill. The North fault cuts ore bodies in the Excess and Rambler mines (Griswold, 1961). The South fault strikes N70–75°E and forms the southern boundary of Mine Hill. Numerous pre-ore faults, striking N40–80°E, are filled with barren, massive quartz. The 914-m-long Crest fault is one of the most prominent of the pre-ore faults and is cut by younger mineralized faults. The Crest fault has <30 m of vertical movement (Griswold, 1961). Many of the mines occur along a swarm of silicified and mineralized, steeply dipping north–northeast-trending normal faults with little if any displacement. The faults on the north side of Mine Hill tend to dip to the north or northwest, similar to the dip of the North fault. The faults on the south side of Mine Hill tend to dip to the south or east, similar to the dip of the South fault. In contrast to the extensive faulting in the Middle, East, and Mine Hills, the volcanic rocks exposed along the Main Ridge are offset by six or seven north-trending normal faults, with minor displacements (Thorman and Drewes, 1980).

GEOCHRONOLOGY OF VICTORIO IGNEOUS ROCKS

A surface sample of the Victorio Peak dacite and three samples from drill cores (two granite samples and an altered mafic sill) were dated using the $^{40}Ar/^{39}Ar$ method. The goals of these analyses were to determine the ages, cooling history, and possibly the timing of mineralization in the Victorio Mountains.

The $^{40}Ar/^{39}Ar$ age spectrum of the Victorio Peak dacite (VIC-1) is given in Figure 7. The age spectrum is complex with ages ranging from ~30–42 Ma and the overall spectrum is significantly younger than the 41.7-Ma zircon-fission-track age reported by Thorman and Drewes (1980). Several of the initial heating steps yield apparent ages which cluster at ~30 Ma and may represent a time of hydrothermal alteration rather than a primary crystallization age in light of the disagreement with the fission track result.

The age spectrum diagrams for the Victorio granite K-feldspar and biotite are shown in Figure 8, and the mafic-sill age spectra and K/Ca diagrams are given in Figure 9. The biotites have slightly disturbed age spectra; however, weighted mean ages calculated for the steps indicated in Figure 8 are indistinguishable at 35.09 ± 0.08 and 35.27 ± 0.41 Ma for samples GG1-2225 and GVM-A1-2741, respectively. The K-feldspars from these samples yield highly discordant age spectra (Fig. 8). Both samples have initial ages which step down to minimum values before climbing to terminal ages ranging from ~50–70 Ma (Fig. 8). The K-feldspars have steps that are both younger and older than the coexisting biotite pairs. The age spectrum for the mafic sill (sample GVM7-1460) is highly complex (Fig. 9). Following two relatively old initial steps, a minimum apparent age of ~36 Ma is reached with the remaining part of the age spectrum exhibiting an overall climb in apparent age to ~600 Ma. The K/Ca values for this sample are quite variable and are highest when apparent ages are lowest (Fig. 9).

MINERAL DEPOSITS

Based on field mapping and examination of drill core, three types of deposits have been found in the Victorio Mountains: (1) carbonate-hosted Pb-Zn replacement, (2) W-Be-Mo skarn/vein, and (3) porphyry Mo deposits. The porphyry Mo deposits are not exposed at the surface and

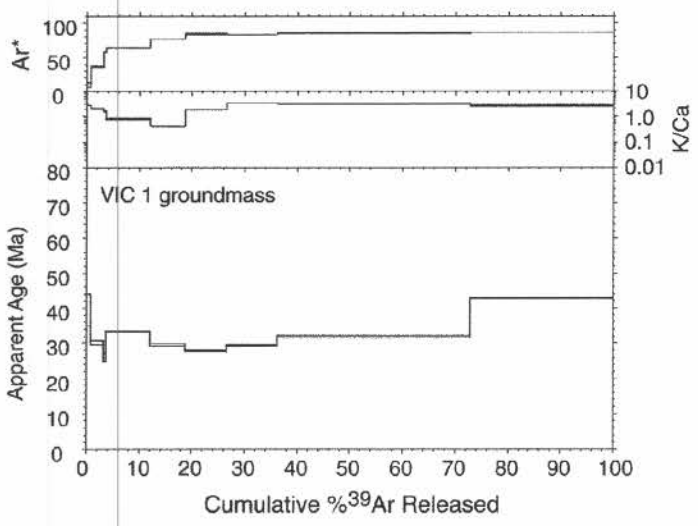

FIGURE 7. Age spectra for groundmass of Victorio Peak dacite (VIC 1).

found only in drill core in the Victorio granite.

The carbonate-hosted Pb-Zn replacement deposits occur as oxidized vein and replacement deposits within Ordovician and Silurian dolostones and limestones at Mine Hill. The deposits include replacements in carbonate rocks with little or no calc-silicate minerals and minor replacement veins in carbonate rocks. They are typically lead/zinc dominant, with by-product copper, silver, and gold (Table 3). Recognizable silver and gold minerals are rare. The more productive deposits in the Victorio district occur along faults or fractures that strike N30–65°E (Fig. 3). Some veins are as much as 274 m long. Brecciation, dissolution, and recrystallization of the dolostones are common in the vicinity of the mineral deposits. The faults exhibit both pre- and post-mineralization movement (Griswold, 1961). Ore minerals include galena, smithsonite, cerussite, and anglesite with rare sphalerite and chalcopyrite in a gangue of quartz, calcite, and iron oxides; other minerals are listed in Table 4. Ore produced from the Rambler mine averaged 12.5% Pb and 3.9% Zn (NMBMMR file data). Gold assays range as high as 5.5 ppm (Table 3; Griswold et al., 1989).

At the surface, the W-Be-Mo skarn/vein deposits occur as small veins and replacement lenses within the Ordovician limestones and dolostones in the vicinity of rhyolite intrusions. In drill core, nearly all of the Ordovician and Cambrian sedimentary rocks are mineralized to some extent. Based on optical examination, ore minerals include helvite, wolframite, scheelite, molybdenite, galena, sphalerite, and beryl in a gangue of quartz, calcite, and local grossularite, tremolite, pyroxene, idocrase, and phlogopite (Table 4; Holser, 1953; Warner et al., 1959; Richter and Lawerence, 1983). More recently, Campbell and Robinson-Cook (1987) found that fluid inclusions in wolframite from the Victorio mining district had temperatures of homgenization of 280–380°C and salinities of 5.4–8.9 eq. wt.% NaCl. Quartz fluid inclusions had temperatures of homgenization of 141–320°C and salinities of 1.3–10 eq. wt.% NaCl.

Several samples of W-Be-Mo skarn/vein deposits from drill cores were examined using the electron microprobe. A diverse mineral assemblage consistent with that observed petrographically was found within the skarn replacement and vein samples. Sulfides and associated metallic phases include molybdenite, pyrite, sphalerite, scheelite-powellite solid solution, galena, and Fe-oxides. Other phases include garnet, a wide compositional range of pyroxene, actinolite, serpentine, phlogopite, calcite, quartz, talc, and fluorite.

Garnet is present both as very large (up to 1 cm) chemically zoned crystals (Fig. 10), and as small crystals intergrown with other phases. Based on qualitative analysis and chemical mapping, both high- and low-Mn garnets are present, and the high-Mn crystals appear to have crystallized before the low-Mn garnets (Fig. 11). Wollastonite and a calcic pyroxene are found in association with garnet. In some cases, virtually an entire vein sample is composed of garnet, with distinct bands of

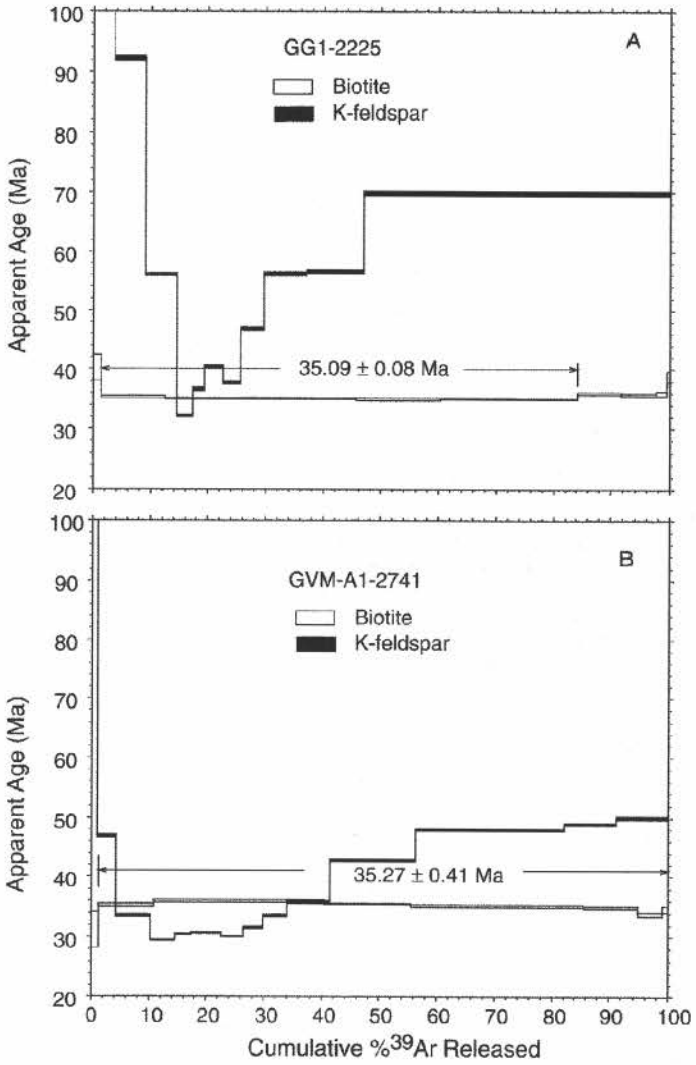

FIGURE 8. Biotite and K-feldspar age spectra for two samples of the Victorio granite.

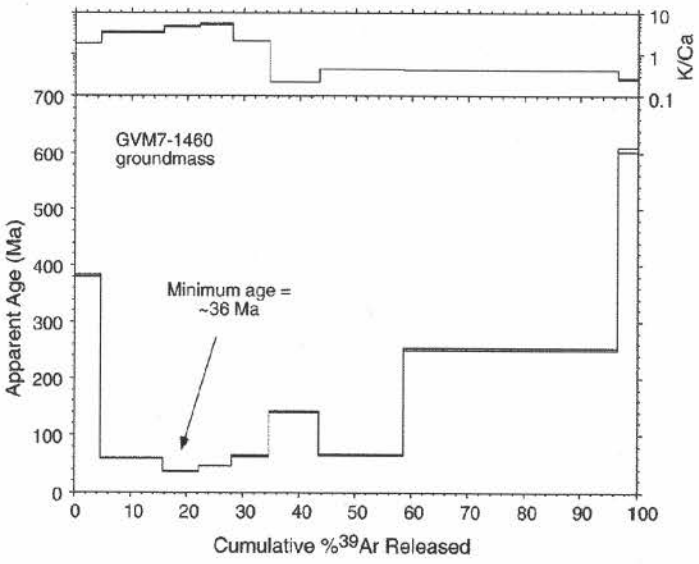

FIGURE 9. Age spectra for groundmass concentrate from mafic sill (sample GVM7-1460).

TABLE 3. Chemical analyses of mineralized samples collected from the Victorio district.

Lab No.	Field No.	Cu ppm	Pb ppm	Zn ppm	Mo ppm	As ppm	Au ppm	Ag ppm	Sample Description
Mine Hill carbonate-hosted Pb-Zn replacement deposits									
158	VIC 3	8200	13,800	22,900	25	1400	1.5	72	3-ft chip across back at portal of Lower Jessie adit
159	VIC 4	130	4900	13,700	<0.5	15,000	1.0	38	grab of pillar at winze in Lower Jessie adit
160	VIC 5	10	52	85	<0.5	47	0.006	<2	grab of rib of vein at Lower Jessie adit
161	VIC 4M	320	39,700	1100	<0.5	730	1.1	120	2-ft chip of vein in Helen mine, 1st level
162	VIC 4B	1000	3300	3500	<0.5	600	0.10	36	4-ft chip across face in Helen mine, 1st level
163	VIC 4C	48,000	8200	171,400	<0.5	460	0.5	15	chip of vein in Helen mine, 1st level
164	VIC 132	141	3700	680	<0.5	420	0.50	35	dump sample, Jessie
165	VIC 34D	1700	49,000	40,000	<0.5	2100	0.50	84	muck sample at 100 ft in Helen mine
166	VIC 34	700	14,800	3200	<0.5	2000	2.7	120	muck sample at 100 ft in Helen mine
167	VIC 144	4000	14,000	9100	<0.5	1300	0.02	13	dump sample, Parole
168	VIC 42	890	14,000	3400	<0.5	990	0.30	21	sample of rib at Excess
169	VIC 48	1400	5400	30,700	3	38	0.05	4	sample of rib at Rover, 1st level
170	VIC 49C	550	1200	1700	<0.5	4100	1.4	50	sample of rib at Rover, 1st level
171	VIC 50B	730	5600	1800	<0.5	1200	0.1	61	grab of muck pile, Rover, 1st level
172	VIC 50	420	22,700	5800	10	3700	0.40	47	sample of rib at Rover, 1st level
173	VIC 80B	890	118,000	95	<0.5	990	0.60	88	dump sample, Rover
Middle Hills W-Be-Mo skarn/veins									
174	VIC 200	42,000	123,000	15,000	10	210	0.50	89	dump sample at Tungsten Hill mine
1710	VIC-19-99	2970	5550	130	<5	1	0.41	61.7	select dump
1711	VIC-26-99	31,885	84,890	20,330	290	47	0.41	778.3	select dump at shaft
1712	VIC-27-99	22,720	22,920	62,970	60	11	0.34	672.0	select dump at shaft
1713	VIC-28-99	11,855	3160	59,080	26	9	<0.17	65.1	select dump at shaft
1714	VIC-35-99	23,740	2790	128,070	<5	255	0.75	30.9	select dump
1716	VIC-40-99	625	3570	5350	<5	<1	<0.17	51.4	select dump of skarn
1715	VIC-41-99	77	480	920	12	2	<0.17	17.1	select dump of skarn, Tungsten shaft

Cu, Pb, Zn analyzed by FAAS at NMBMMR Chemical laboratories. Samples 158–173 collected at Mine Hill (carbonate-hosted Pb-Zn replacement deposits) and samples 174, 1709–1716 collected at Middle Hills (W-Be-Mo skarn/vein deposits). Sample locations are in Figure 2. For samples 158–174, Au and Ag analyzed by ICP-AES by USGS laboratories. For samples 1709–1716, Au and Ag analyzed by fire assay methods at NMBMMR. — not analyzed. The samples were analyzed at more than one laboratory, and hence presentation of analytical uncertainties and detection limits are not made here. These analyses should be used as rough indications of composition only.

other mineral phases, both metal-bearing and non-metal-bearing, at the outer margins of the vein. Included in these veins are diamond-shaped amphibole crystals up to 500 μm in length (Fig. 12). Based on backscatter electron imaging and X-ray mapping, these amphibole crystals are compositionally zoned, and contain proportionately more Fe in their cores and more Mg in their rims. In other areas, amphibole is present as thin, bladed–acicular crystal masses that appear to have formed as open-space filling (Fig. 13). Blocky fluorite crystals, as well as orthoclase and albitic plagioclase, are commonly found in association with the amphibole. The fluorite appears to have formed after amphibole crystallization. Another common phase in the samples is phlogopite, which forms the small, indistinct groundmass of some parts of samples, but is also present as radiating clusters of acicular crystals that appear to have formed in open spaces left during garnet or amphibole precipitation (Figs. 10, 11). The open-space-filling phlogopite is found associated with serpentine and quartz (Fig. 14). Calcite is found widely dispersed throughout the samples, and talc and chlorite have been identified in some samples.

A wide range of sulfides and other metallic minerals are observed in the skarn samples (Table 4), and these were also examined using the microprobe. These include euhedral rods or masses of molybdenite, sphalerite, fine galena, a blocky iron sulphide, probably pyrite, Fe oxides, blocky masses of scheelite (CaWO4), powellite (CaMoO4) (Fig. 15), and a more-or-less complete solid solution between scheelite and powellite. The Fe oxides are typically finely dispersed throughout the sample. These metal-bearing minerals are more abundant in the samples that show a distinct vein morphology as compared to the skarn replacement samples. In some samples, distinct bands of concentrated metal-

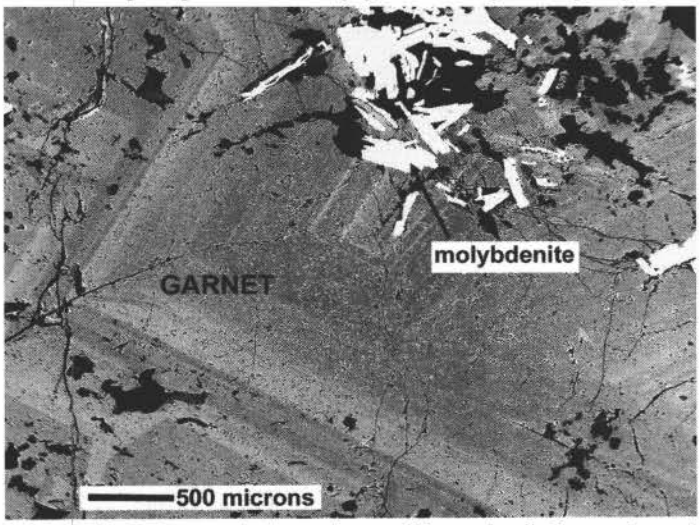

FIGURE 10. Backscattered electron image of large, chemically-zoned garnet crystals associated with molybdenite in a vein cutting El Paso Group limestone. The gray-scale banding in the garnet crystals is indicative of chemical variation.

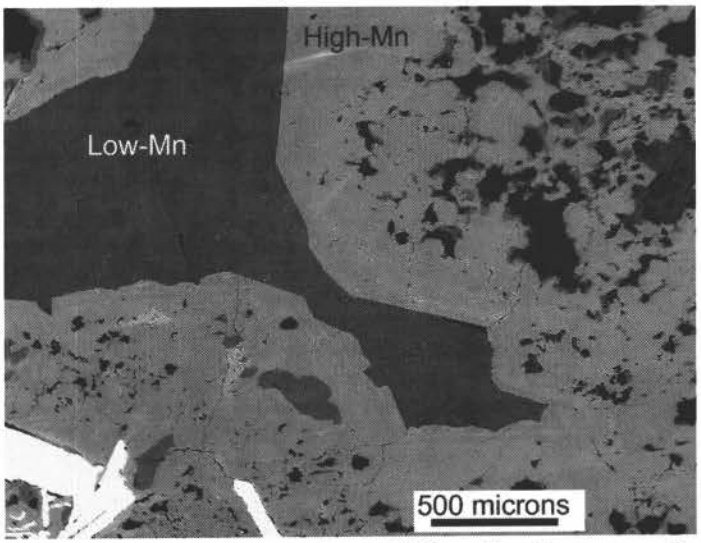

FIGURE 11. Backscattered electron image of high- and low-Mn garnet crystals in a vein cutting El Paso Group limestone.

TABLE 4. Selected minerals found in the Victorio mining district (from Holser, 1953; Griswold, 1961; DeMark, 1992; Northrop and LaBruzza, 1996; Beyer, 1997; Gulf Minerals company reports; this study).

MINERAL	CHEMICAL FORMULA	MINERAL	CHEMICAL FORMULA
SILICATES		**SULFIDES, SULFATES, METALS**	
Chondrodite (2)	$(Mg, Fe)_5(SiO_4)_2(F, OH)_2$	**Pyrrhotite** (1, 2, 3)	FexS
Humite (2)	$(Mg, Fe)_7(SiO_4)_3(F, OH)_2$	**Marcasite** (1, 2)	FeS_2
Clinohumite	$(Mg, Fe)_9(SiO_4)_4(F, OH)_2$	Pyrite (1, 2, 3)	FeS_2
Helvite (2)	$Mn_4Be_3(SiO_4)_3S$	**Chalcopyrite** (1, 2)	$CuFeS_2$
Danalite (2)	$Fe_4Be_3(SiO_4)_3S$	Bornite (1)	Cu_5FeS_4
Willemite (1)	Zn_2SiO_4	Tetrahedrite (2?)	$(Cu,Fe)_{12}Sb_4S_{13}$
Zircon (3)	$ZrSiO_4$	Sphalerite (1, 2)	(Zn, Fe)S
Garnet (2, 3)	Range of compositions	**Wurtzite** (1)	(Zn,Fe)S
Allanite (3)	$(Y, Ce, Ca)_2(Al, Fe)_3(SiO_4)_3(OH)$	Molybdenite (2, 3)	MoS_2
Beryl (2, 3)	$Be_3Al_2Si_6O_{18}$	Gold (1)	Au
Diopside (2)	$CaMgSi_2O_6$	Argentite (1)	Ag_2S
Augite (2)	$(Ca,Na)(Mg,Fe,Al,Ti)(Si,Al)_2O_6$	Chlorargyrite (1)	AgCl
Tremolite (2)	$Ca_2(Mg,Fe)_5Si_8O_{22}(OH)_2$	Galena (1, 2)	PbS
Phlogopite (2)	$KMg_3Si_3AlO_{10}(F, OH)_2$	Anglesite (1)	$PbSO_4$
Serpentine (2)	$(Mg, Fe, Ni)_3Si_2O_5(OH)$	Friedrichite (1)	$Pb_5Cu_5Bi_7S_{18}$
Talc (2)	$Mg_3Si_4O10(OH)_2$	**Galenobismutite** (2, 3)	$PbS(Bi_2S_3$
Hemimorphite (1)	$Zn_4Si_2O_7(OH)_2(H_2O$	**Bismuthinite** (2, 3)	Bi_2S_3
Quartz (1, 2, 3)	SiO_2		
Scapolite (2)	$(Na,Ca)_4Al_{3-6}Si_{6-9}O_{24}$ (Cl,CO_3,SO_4)	**OXIDES**	
		Adamite (1)	$Mg_5B_{12}O_{20}(15H_{2O}$
CARBONATES		Psilomelane (1, 2)	Mn oxide
Calcite (1, 2, 3)	$CaCO_3$	Magnetite (2, 3)	Fe_3O_4
Rhodochrosite (3)	$MnCO_3$	**Cassiterite** (2?)	SnO_2
Reevesite (1)	$Ni_6Fe_2(CO_3)(OH)_{16}.4H_2O$	Wulfenite (1, 2)	$PbMoO_4$
Smithsonite (1)	$ZnCO_3$	Vanadinite (1, 2)	$Pb_5(VO_4)_3Cl$
Cerussite (1)	$PbCO_3$	Mimetite (1)	$Pb_5(AsO_4)_3Cl$
Beyerite (2)	$(Ca, Pb)Bi_2(CO_3)2O_2$	Descloizite (1)	$PbZn(VO_4)(OH)$
Bismutite (2)	$Bi_2(CO_3)O_2$		
Aurichalcite (1)	$(Zn,Cu)_5(CO_3)_2(OH)_6$	**OTHER**	
Kettnerite (1)	$CaBi(CO_3)OF$	Fluorite (2, 3)	CaF_2
		Kolfanite (1)	$Ca_2Fe_3O_2(AsO_4)_3(2H_2O$
TUNGSTATES		Bromargyrite (1)	AgBr
Scheelite (2)	$CaWO_4$	Carminite (1)	$PbFe_2(AsO_4)_2(OH)_2$
Powellite (2)	$CaMoO_4$	Beudantite (1)	$PbFe_3(As,O_4)(SO_4)(OH)_6$
Hübnerite (2)	$MnWO_4$	Pyromorphite (1)	$Pb_5(PO_4)_3Cl$
Wolframite (1, 2)	$(Fe, Mn)WO_4$		
Stolzite (2)	$PbWO_4$		

Minerals in bold are newly reported in this study. Type of deposit in parenthesis: 1—carbonate-hosted Pb-Zn replacement deposits, 2—Be-Mo-W skarn/vein deposits, and 3—porphyry Mo deposits.

bearing phases are present along vein margins, suggesting intervals of favorable conditions for ore formation during the growth of the veins. However, in other samples, the metal-bearing minerals are dispersed throughout the sample.

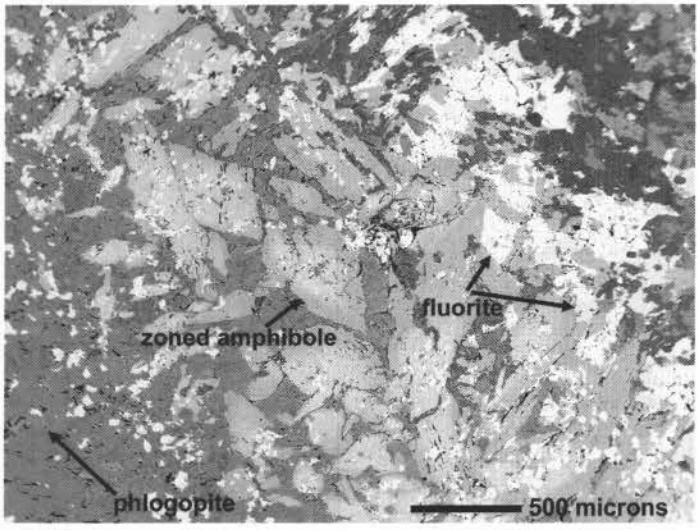

FIGURE 12. Backscattered electron image of diamond-shaped, zoned amphibole crystals, phlogopite and fluorite in a vein cutting El Paso Group limestone. The gray-scale variation in the amphibole is indicative of Fe to Mg zonation from the cores to the rims.

The distribution and composition of W-Be-Mo skarn/vein deposits appear to be stratigraphically controlled. In the Bliss Formation, the three major lithologies have distinct differences in Mo-W ratios, vein thickness and vein density. Lenses of dense mineralization occur in

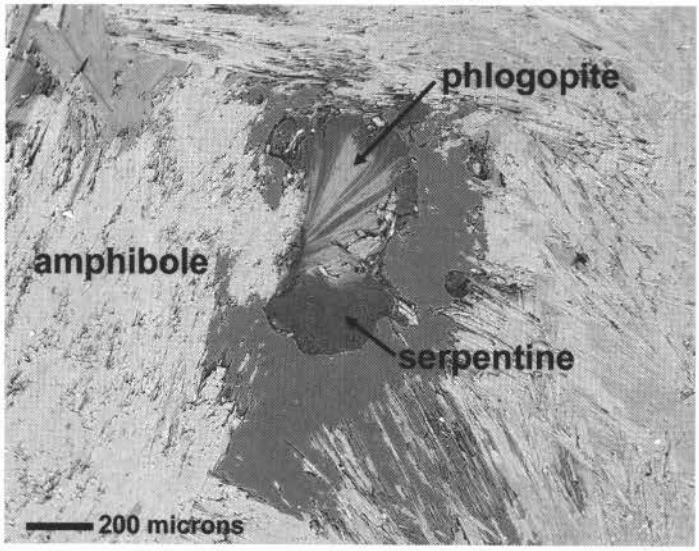

FIGURE 13. Backscattered electron image of amphibole matrix with phlogopite, serpentine, and quartz open space filling in a carbonate-replaced zone in El Paso Group limestone.

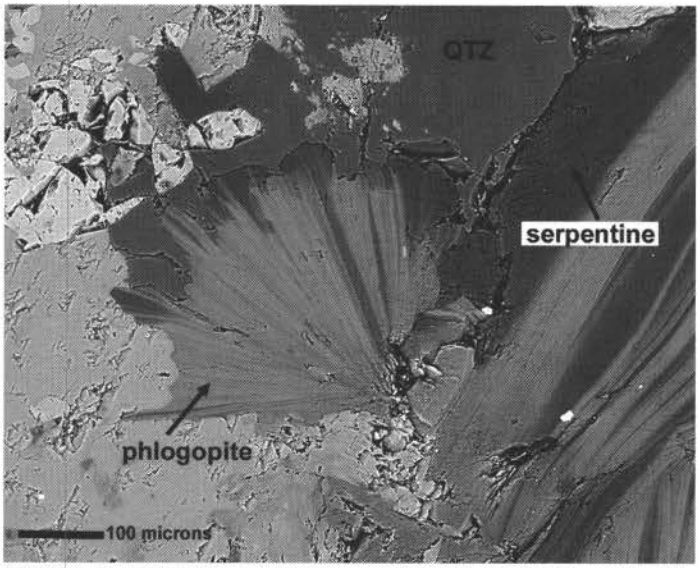

FIGURE 14. Backscattered electron image of garnet and fluorite matrix with phlogopite, serpentine, and quartz open-space filling in a carbonate-replaced zone in El Paso Group limestone.

some Bliss lithologies, whereas others are nearly barren. The calcium-poor orthoquartzite contains very little scheelite, which occurs as thin veinlets. The silty glauconitic facies is richer in calcium and has intermediate tungsten values. The molybdenite in this facies is vein-controlled while the scheelite is predominantly disseminated. The silty limestone facies contains enough calcium to precipitate significant disseminated scheelite. The veins in this facies are thicker and more common. Molybdenum mineralization is primarily vein-controlled with minor dissemination. There is also a strong positive correlation between disseminated and vein-controlled W-Mo mineralization and disseminated fluorite mineralization (Heidrick, 1983).

Gulf Minerals Resources, Inc. drilled 71 drill holes northwest of Mine Hill and found a subeconomic Mo-W-Be deposit at depths ranging from 274 to 457 m. Ore minerals include molybdenite, powellite, scheelite, beryl, helvite, bismuthinite, and wolframite (Table 3).

Two small copper-veins cut dacite flows on the Main Ridge in the Victorio Mountains and are the only mineralized zones encountered north of the Victorio Mountains fault. The veins are <1m wide, a few meters long, and consist of calcite, quartz, malachite, azurite, and trace amounts of oxidized pyrite. They strike N40–45°E and are steeply dipping.

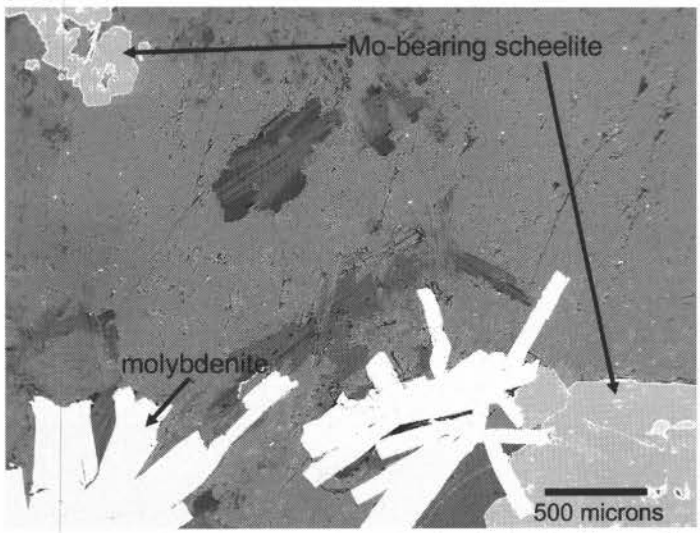

FIGURE 15. Backscattered electron image of a phase in the scheelite-powellite solid-solution series, as well as bright, tabular molybdenite crystals in a vein-cutting El Paso Group limestone.

ALTERATION

Four types of alteration occur in the Victorio mining district: contact-metasomatic non-mineralized skarn, silicification (veins and jasperoids), sericitic/argillic, and carbonate recrystallization. Contact-metasomatic alteration produced extensive skarns in carbonate units below the Fusselman Dolomite in the district, some of which are exposed at the surface in the Middle Hills. The contact-metasomatic alteration appears to be related to the rhyolite and mafic dikes and sills and to the buried Victorio granite. The most intense amount of contact-metasomatic alteration is in the Middle Hills and skarn alteration appears to decrease south towards Mine Hill, where there is no skarn alteration at the surface or reported in underground workings or drill core.

Two types of silica deposition occur in the district, manifested by quartz veins and jasperoids. Massive quartz veins fill pre-ore faults at Mine Hill. Silicification commonly occurs along veins and joints and along the Victorio Mountains fault in the Middle Hills. Quartz veining is intimately associated with the carbonate-hosted Pb-Zn replacement deposits and may be the main mechanism of ore emplacement at Mine Hill. Silica replacement occurs within the carbonate units along bedding planes and in breccia pipes.

Sericitic/argillic alteration consists of sericite, adularia, chlorite, and clay minerals and appears to be confined predominantly to igneous rocks. Nearly all of the mafic rocks are altered to sericite, chlorite, and clay. The "felsite" dike along the Mine Hill fault and some of the Lower Cretaceous volcaniclastic strata have been altered as well. Minor quartz veining and iron staining commonly accompanies the sericitic/argillic alteration.

Carbonate recrystallization is common in, and adjacent to, all mineralized areas in the district. Some carbonate recrystallization may be related to karsting that occurred before intrusion of the igneous rocks and subsequent mineralization. In many areas, white marble is locally common. Other carbonate recrystallization is related to quartz and jasperoid veins. The amount of carbonate recrystallization is related to the size and intensity of the vein (Wessel and Maciolek, 1989).

The alteration and mineralization at Middle Hills is restricted to the faults cutting the Fusselman Dolomite, Upham Dolomite, and El Paso Group. Pink jasperoid, recrystallized limestone, and marble are locally common in discontinuous pods along the faults. Locally, pyrite, malachite, brochantite, chrysocolla, chalcocite, and smithsonite occur as disseminations or small spotty pods within the altered dolostone. Quartz is typically very fine grained and only locally is crystalline vein quartz found.

DISCUSSION

Age of granite emplacement and mineralization

The age-spectra complexity does not allow unambiguous age interpretation. Generally $^{40}Ar/^{39}Ar$ biotite ages from granitoids are interpreted to coincide with the time that the rock cooled below 300–350°C (McDougall and Harrison, 1999). However, the fact that parts of the K-feldspar age spectra are both younger and older than the biotite could indicate that the biotite plateau ages are not geologically relevant. Alternatively, the old parts of the K-feldspar spectra may be caused by excess argon and the younger parts of their spectra related to their lower argon retentivity relative to biotite.

Age gradients in K-feldspar age spectra are known to be related to argon loss from variably retentive diffusion domains during slow-cooling and/or episodic reheating (Lovera et al., 1989; McDougall and Harrison, 1999). Also, steep age increases for the later part of K-feldspar age spectra can be caused by excess argon incorporation into large diffusion domains (Foster et al., 1990). The complexity of K-feldspar from GG1-2225 (Fig. 8) may be excess argon in large diffusion domains, however the gradual climb in age shown by GVM-A1-2741 K-feldspar (Fig. 8) is a very common age spectrum and not typically ascribed to excess argon. Thus, two end-member possibilities appear to be viable to explain the argon results from the Victorio granite. The granite may be ~35 Ma (biotite plateau age) and cooled below ~175°C by ~30 Ma (lower age of K-feldspar spectrum), or the granite is signif-

icantly older (>70 Ma) and was reheated at 30–35 Ma ago. Age gradients caused by partial argon loss will not generally be recorded by biotite-age spectra due to the loss of the spatial argon distribution information caused by catastrophic degassing in the laboratory. Thus, the biotite ages could be intermediate between the intrusion age and the time of later argon loss. Under this scenario, a reheating event at 30 Ma may be recorded by K-feldspar GVM-A1-2741 and the 35-Ma biotite ages represent partial argon loss with no specific chronological significance. If the biotite plateau ages are accurate with respect to the intrusion age of the Victorio granite, then the older ages recorded by the K-feldspars would be interpreted as caused by excess argon. The younger ages recorded by the K-feldspars would indicate protracted cooling of the granite to about 175°C by ~30 Ma. This being the case, the granite must have been emplaced at significant depth (>5 km).

The age spectrum complexity of groundmass sample GVM7-1460 (Fig. 9) does not provide specific age information. Electron microprobe analyses reveal distinct zones and rims of adularia. Argon from the adularia is dominating the initial parts of the age spectrum and the minimum age of 36 Ma is a maximum age for the cooling and argon retention of the adularia. That the Victorio granite samples recorded ages in the approximate range of this adularia may indicate that the alteration observed in GVM7-1460 is related to emplacement of the granite. Alternatively, the adularia age may be the geological representation of the heating event that affected the Victorio granite.

Patterns of mineralization and relationships between types of mineralization

The general paragenetic sequence of the carbonate-hosted Pb-Zn replacement deposits began with the formation of the jasperoids and massive quartz veins filling pre-ore faults. Small amounts of galena and chalcocite occur in quartz at the Jessie mine and probably represent the first mineralizing event. Faulting continued after the first stage and was followed by a second stage of multiple episodes of Pb-Zn replacement veins. Relatively more quartz appears to precipitate early in the mineralization sequence. However, barren quartz and calcite were the last phases deposited during primary mineral deposition. Subsequent oxidation or supergene enrichment occurred.

Mineralogical investigations of samples from skarn vein and replacement deposits, as well igneous granite, provide some insight into the processes of skarn formation. The assemblages present in the samples that appear to be skarn replacement deposits are indistinguishable from those that are veins, and appear to represent the same mineralization event. The mineral assemblage, particularly the presence of serpentine, magnesian pyroxene, phlogopite, and talc, and the absence of wollastonite and apatite suggests that the Victorio Mountains skarn system should be classified as magnesian, rather than calcic (e.g., Kwak, 1994). The presence of fluorite further suggests that the skarn-related fluids were fluorine-rich.

Mineralogy and textural relationships observed in both skarn replacement and vein deposits suggest that remnants of a primary, or prograde, skarn assemblage are present, as well as a number of secondary, or retrograde phases. Kwak (1994) suggests that in a magnesian skarn, garnet and pyroxene ± magnetite make up the primary or prograde assemblage, whereas the secondary or retrograde assemblages occur in the following order:

(1) Ca-Mg amphibole ± calcite ± sulfides ± magnetite
(2) talc ± calcite ± sulfides
(3) phlogopite ± sulfides
(4) serpentine ± calcite ± sulfides
(5) chlorite ± calcite or quartz ± sulfides

In one sample, large (~1 cm) complexly zoned garnets, interpreted to be part of a prograde skarn assemblage, are present in an open-space-filling vein (Fig. 10). In a nearby part of the same sample, smaller garnets co-exist with phlogopite, serpentine and talc, the latter interpreted to be part of a retrograde facies. Other samples record similar ranges of mineral phases. In some cases, delicate, fan-shaped masses of phlogopite appear to have crystallized in open-space cavities in either a garnet- or amphibole-rich matrix. Although the amphibole may be related to early retrograde mineralization, the intragranular cavities in the garnet matrix probably formed during prograde skarn evolution. Serpentine and quartz formed around and intergrown with the phlogopite; both minerals would form later in prograde evolution than phlogopite. Hence, the skarn replacement and vein samples from Victorio Mountains appear to record an extended history of skarn formation, spanning a range of fluid compositions and/or formation temperatures.

One outstanding question in the Victorio mining district is the relationship between the three major episodes of igneous intrusion and the mineralization. The carbonate-hosted Pb-Zn replacement deposits in the Victorio district are epithermal deposits as evidenced by ore textures, ore controls, and correlations with similar carbonate-hosted replacement deposits in southwestern New Mexico, which are also believed to be epithermal. More concrete evidence for association between igneous and mineralizing activity comes from microprobe analysis of minerals in the Victorio granite and a spatially-associated skarn provide some evidence for such a relationship. The Victorio skarn deposits contain abundant fluorite, apparently coprecipitated with other skarn minerals (Fig. 12) suggesting that the skarn-forming fluids were F-rich. The Victorio granite also contains fluorite as apparently-primary inclusions in garnet, suggesting that the magma which formed this granite was F-rich. Although fluorine does not fractionate into a magmatic vapor phase as readily as Cl, partition coefficients for F are higher than 1 kbar for a water-saturated, peraluminous granitic melt at 800°C and 2 kbar (Webster, 1990). Therefore, a F-rich granitic melt could be expected to generate a fluid phase that would create a F-bearing skarn. Furthermore, Mn-rich garnets are present in both the granite and the skarn, providing a further indirect geochemical link between the two.

SUMMARY AND FUTURE DIRECTIONS

The Victorio mining district is characterized by complex stratigraphy and structural geology, three types of mineral deposits as well as several episodes of igneous intrusions. Due to the recent availability of subsurface data and drill core from the Victorio district, refinements to the stratigraphy and structural geology have been possible. Furthermore, these samples and data have allowed better understanding of the geochemistry and the relationship between some of the mineralization and igneous intrusions. The skarn/veins appear related to the intrusion of the Victorio granite as evidenced by spatial association, similar composition of garnets found in both deposits, and presence of fluorite in both systems. Geochronological analysis of igneous samples suggests that intrusions may have occurred at around 35 Ma, and/or igneous rocks may have been reheated at around 35 Ma. The presence of 35-Ma adularia in one of the igneous samples suggests that high-temperature alteration and mineralization may have taken place around that time, providing a very tentative suggestion that at least some of the Victorio mining district mineralization occurred then.

Important questions remain to be fully answered about the geology of the Victorio-mining-district area. What is the nature of the Victorio Mountain and Main Ridge faults and are they related to the igneous intrusions and subsequent mineralization? What are the emplacement ages of the intrusions? What are the genetic relationships between the three types of mineral deposits? Is there an overall zoning pattern within the district? Are the carbonate-hosted replacement deposits an outer epithermal zone related to the magmatic-hydrothermal porphyry Mo deposit or were they formed during a separate mineralizing event? Future endeavors, including mapping, fluid inclusion analyses, stable isotope analyses, mineral chemistry, and additional age dating will address these issues.

ACKNOWLEDGMENTS

This paper is part of a study of the mineral resources of the Mimbres Resource Area (Doña Ana, Luna, Hidalgo, and Grant Counties), in cooperation with the USGS and U.S. Bureau of Land Management. Susan Bartsch-Winkler, Homer Milford, David Sutphin, James

McLemore, and Chuck O'Donnell are acknowledged for field assistance, discussions, and providing data. Homer Milford also provided some of the historical data on the district. Lone Mountain Mining Co. and Leonard Resources donated drill core and subsurface information. Chris McKee (NMBMMR) analyzed some samples by X-ray-fluorescence using the Phillips PW 2400 instrument purchased with funds from NSF grant EAR-9316467. The Cameca SX-100 electron microprobe at NMIMT was partially funded by NSF Grant STI-9413900. Lynn Brandvold and Ibrahim H. Gundiler (NMBMMR Chemistry Laboratory) analyzed some samples for Au, Ag, Cu, Pb, Zn, As, Mo, and Sb. Frank Kottlowski and Andrew Campbell reviewed an earlier draft of this manuscript and their comments are appreciated. This work is part of ongoing research of mineral resources in New Mexico at NMBMMR, Peter Scholle, Director and State Geologist.

REFERENCES

Bell, A. R., 1983, Victorio Mountain molybdenum/tungsten project, Luna County, New Mexico: Gulf Mineral Resources Co., unpublished report on file at the Anaconda Geological Document Collection, American Heritage Center, University of Wyoming, n. 43303.01, 150 p.

Beyer, J., 1997, A second New Mexico carminite locality, Victorio Mountains, Luna County, New Mexico (abs.): New Mexico Geology, v. 19, p. 26–27.

Campbell, A. and Robinson-Cook, S., 1987, Infrared fluid inclusion microthermometry on coexisting wolframite and quartz: Economic Geology, v. 82, p. 1640–1645.

Corbitt, L. L. and Woodward, L. A., 1970, Thrust faults of the Florida Mountains, New Mexico and their regional tectonic significance: New Mexico Geological Society, Guidebook 21, p. 69–74.

Dale, V. B. and McKinney, W. A., 1959, Tungsten deposits of New Mexico: U.S. Bureau of Mines, Report of Investigations 5517, 72 p.

DeMark, R., 1992, New Mexico mineral locality index: Rocks and Minerals, v. 67, p. 314–327, 330–331.

Drewes, H., 1991, Description and development of the Cordilleran orogenic belt in the southwestern United States: U.S. Geological Survey, Professional Paper 1512, 92 p.

Elston, W. E., 1958, Burro uplift, northeastern limit of sedimentary basin of southwestern New Mexico and southeastern Arizona: American Association of Petroleum Geologists Bulletin, v. 42, p. 2513–2517.

Foster, D. A., Harrison, T. M., Copeland, P. and Heizler, M. T., 1990, Effects of excess argon within large diffusion domains on K-feldspar age: Geochimica et Cosmochimica Acta, v. 54, p. 1699–1708.

Griswold, G. B., 1961, Mineral deposits of Luna County, New Mexico: New Mexico Bureau of Mines and Mineral Resources, Bulletin 72, 157 p.

Griswold, G. B., Boy, R., Olson, R. R. and Zrinscak, P., 1989, Reconnaissance gold geochemical survey of five selected areas in southwestern New Mexico: New Mexico Bureau of Mines and Mineral Resources, Open-file Report OF-357, 19 p.

Heidrick, T., 1983, Victorio project geologic report: unpublished report to Gulf Mineral Resources Co., on file at New Mexico Bureau of Mines and Mineral Resources archives, 141 p.

Holser, W. T., 1953, Beryllium minerals in the Victorio Mountains, Luna County, New Mexico: American Mineralogist, v. 38, p. 599–611.

Jones, F. A., 1904, New Mexico mines and minerals (World's Fair edition): Santa Fe, 349 p.

Kottlowski, F. E., 1960, Summary of Pennsylvanian sections in southwestern New Mexico and southeastern Arizona: New Mexico Bureau of Mines and Mineral Resources, Bulletin 66, 187 p.

Kottlowski, F. E., 1963, Paleozoic and Mesozoic strata of southwestern and south-central New Mexico: New Mexico Bureau of Mines and Mineral Resources, Bulletin 79, 100 p.

Kwak, T. A. P., 1994, Hydrothermal alteration in carbonate-replacement deposits: ore skarns and distal equivalents; *in* Lentz, D. R., ed., Alteration and alteration processes associated with ore-forming systems: Geological Association of Canada, Short Course Notes, v. 11, p. 381–402.

Lawton, T. F., Basbilvazo, G. T., Hodgson, S. A., Wilson, D. A., Mack, G. H., McIntosh, W. C., Lucas, S. G. and Kietzke, K. K., 1993, Laramide stratigraphy of the Little Hatchet Mountains, southwestern New Mexico: New Mexico Geology, v. 15, p. 9–15.

Lawton, T. F. and Clemons, R. E., 1992, Klondike basin—late Laramide depocenter in southern New Mexico: New Mexico Geology, v. 14, p. 1–7.

Lindgren, W., Graton, L. C. and Gordon, C. H., 1910, The ore deposits of New Mexico: U.S. Geological Survey, Professional Paper 68, 361 p.

Lovera, O. M., Richter, F. M. and Harrison, T. M., 1989, The $^{40}Ar/^{39}Ar$ geothermometry for slowly cooled samples having a distribution of diffusion domain sizes: Journal of Geophysical Research, v. 94, p. 17,917–17,935.

Lowell, J. D., 1974, Regional characteristics of porphyry copper deposits of the southwest: Economic Geology, v. 69, p. 601–617.

Lucas, S. G., Estep, J. W. and Anderson, B. G., 2000, Lower Cretaceous stratigraphy and biostratigraphy in the Victorio Mountains, Luna County, New Mexico; *in* Lucas, S. G., ed., New Mexico's fossil record 2: New Mexico Museum of Natural History and Science, Bulletin 16, p. 63–72.

Mack, G. H. and Clemons, R. E., 1988, Structural and stratigraphic evidence for the Laramide (early Tertiary) Burro uplift in southwestern New Mexico: New Mexico Geological Society, Guidebook 39, p. 59–66.

Mack, G. H., Kollins, W. B. and Galemore, J. A., 1986, Lower Cretaceous stratigraphy, depositional environments, and sediment dispersal in southwestern New Mexico: American Journal of Science, v. 286, p. 309–331.

McDougall, I. and Harrison, T.M., 1999, Geochronology and thermochronology by the $^{40}Ar/^{39}Ar$ method, 2nd ed.: Oxford University Press, New York, N.Y., , 269 p.

McLemore, V. T., 1993, Geology and geochemistry of the mineralization and alteration in the Steeple Rock district, Grant County, New Mexico and Greenlee County, Arizona [Ph.D. dissertation]: El Paso, University of Texas; also New Mexico Bureau of Mines and Mineral Resources, Open-file Report 397, 526 p.

McLemore, V. T. and Lueth, V. W., 1995, Carbonate-hosted lead/zinc deposits in New Mexico (abs.): International Field Conference on Carbonate-hosted Lead-Zinc Deposits, Society of Economic Geologists, Extended Abstracts, p. 209–211.

McLemore, V. T. and Lueth, V. W., 1996, Lead-zinc deposits in carbonate rocks in New Mexico; *in* D. F. Sangster, ed., Carbonate-hosted lead-zinc deposits: Society of Economic Geologists, 76th Anniversary Volume, Special Publication 4, p. 264–279.

McLemore, V. T., McMillan, N. J., Heizler, M. and McKee, C., 1999, Cambrian alkaline rocks at Lobo Hill, Torrance County, New Mexico—more evidence for a Cambrian-Ordovician aulacogen: New Mexico Geological Society, Guidebook 50, p. 247–253.

McLemore, V. T., Sutphin, D. M., Hack, D. R. and Pease, T. C., 1996, Mining history and mineral resources of the Mimbres Resource Area, Doña Ana, Luna, Hidalgo, and Grant Counties, New Mexico: New Mexico Bureau of Mines and Mineral Resources, Open-file Report 424, 251 p.

Muehlberger, W. R., 1980, Texas lineament revisited: New Mexico Geological Society, Guidebook 31, p. 113–121.

Northrop, S. A. and LaBruzza, F. A., 1996, Minerals of New Mexico: University of New Mexico Press, Albuquerque, New Mexico, 356 p.

Richter, D. H. and Lawrence, V. A., 1983, Mineral deposit map of the Silver City 1° x 2° quadrangle, New Mexico and Arizona: U.S. Geological Survey, Miscellaneous Investigations Series Map I-1310B, scale 1:250,000.

Schmitt, H. A., 1966, The porphyry copper deposits in their regional setting; *in* Titley, S. R. and Hicks, C. L., eds., Geology of the porphyry copper deposits, southwestern North America: The University of Arizona Press, Tucson, p. 17–33.

Thorman, C. H. and Drewes, H., 1980, Geologic map of the Victorio Mountains, New Mexico: U.S. Geological Survey, Miscellaneous Field Studies Map MF-1175, scale 1:24,000.

Turner, G. L., 1962, The Deming axis, southeastern Arizona, New Mexico, and Trans-Pecos Texas: New Mexico Geological Society, Guidebook 13, p. 59–71.

U.S. Bureau of Mines, 1927–1990, Minerals yearbook: Washington, D.C., U.S. Government Printing Office, variously paginated.

U.S. Geological Survey, 1902–1927, Mineral resources of the United States (1901–1923): Washington, D.C., U.S. Government Printing Office, variously paginated.

Warner, L. A., Holser, W. T., Wilmarth, V. R. and Cameron, E. N., 1959, Occurrence of non-pegmatite beryllium in the United States: U.S. Geological Survey, Professional Paper 318, 198 p.

Webster, J. D., 1990, Partitioning of F between H_2O and CO_2 fluids and topaz rhyolite melt: Contributions to Mineralogy and Petrology, v. 104, p. 424–438.

Wertz, J. B., 1970a, Arizona's copper province and the Texas lineament: Mining Engineering, v. 5, p. 80–81.

Wertz, J. B., 1970b, The Texas lineament and its economic significance in southeastern Arizona: Economic Geology, v. 65, p. 166–181.

Wessel, G. R. and Maciolek, J., 1989, An evaluation of the Mine Hill area, Victorio Mountains, Luna County, New Mexico: Potential for undiscovered metallic mineralization: unpublished report to Santa Fe Pacific Mining, Inc., on file at New Mexico Bureau of Mines and Mineral Resources archives, 52 p.